Maximum modulation of plasmon-guided modes by graphene gating

Radko, Ilya; Bozhevolnyi, Sergey I.; Grigorenko, Alexander N.

Published in:
Optics Express

Link to article, DOI:
10.1364/OE.24.008266

Publication date:
2016

Document Version
Publisher's PDF, also known as Version of record

Maximum modulation of plasmon-guided modes by graphene gating

Ilya P. Radko,[1,2,*] **Sergey I. Bozhevolnyi,**[2] **and Alexander N. Grigorenko**[3]

[1]*Department of Physics, Technical University of Denmark, 2800 Kongens Lyngby, Denmark*
[2]*Centre for Nano Optics, University of Southern Denmark, 5230 Odense, Denmark*
[3]*School of Physics and Astronomy, University of Manchester, Manchester M13 9PL, UK*
[*]*iradko@fysik.dtu.dk*

Abstract: The potential of graphene in plasmonic electro-optical waveguide modulators has been investigated in detail by finite-element method modelling of various widely used plasmonic waveguiding configurations. We estimated the maximum possible modulation depth values one can achieve with plasmonic devices operating at telecom wavelengths and exploiting the optical Pauli blocking effect in graphene. Conclusions and guidelines for optimization of modulation/intrinsic loss trade-off have been provided and generalized for any graphene-based plasmonic waveguide modulators, which should help in consideration and design of novel active-plasmonic devices.

OCIS codes: (240.6680) Surface plasmons; (230.2090) Electro-optical devices; (130.4110) Modulators; (250.5403) Plasmonics.

References and links

1. M. Liu, X. Yin, E. Ulin-Avila, B. Geng, T. Zentgraf, L. Ju, F. Wang, and X. Zhang, "A graphene-based broadband optical modulator," Nature **474,** 64–67 (2011).
2. J.-L. Kou, J.-H. Chen, Y. Chen, F. Xu, and Y.-Q. Lu, "Platform for enhanced light-graphene interaction length and miniaturizing fiber stereo devices," Optica **1,** 307–310 (2014).
3. D. Ansell, I. P. Radko, Z. Han, F. J. Rodriguez, S. I. Bozhevolnyi, and A. N. Grigorenko, "Hybrid graphene plasmonic waveguide modulators," Nat. Commun. **6,** 8846 (2015).
4. B. D. Thackray, P. A. Thomas, G. H. Auton, F. J. Rodriguez, O. P. Marshall, V. G. Kravets, and A. N. Grigorenko, "Super-narrow, extremely high quality collective plasmon resonances at telecom wavelengths and their application in a hybrid graphene-plasmonic modulator," Nano Lett. **15,** 3519–3523 (2015).
5. F. Wang, Y. Zhang, C. Tian, C. Girit, A. Zettl, M. Crommie, and Y. R. Shen, "Gate-variable optical transitions in graphene," Science **320,** 206–209 (2008).
6. A. N. Grigorenko, M. Polini, and K. S. Novoselov, "Graphene plasmonics," Nat. Photonics **6,** 749–758 (2012).
7. R. R. Nair, P. Blake, A. N. Grigorenko, K. S. Novoselov, T. J. Booth, T. Stauber, N. M. R. Peres, and A. K. Geim, "Fine structure constant defines visual transparency of graphene," Science **320,** 1308 (2008).
8. L. Song, L. J. Ci, H. Lu, P. B. Sorokin, C. H. Jin, J. Ni, A. G. Kvashnin, D. G. Kvashnin, J. Lou, B. I. Yakobson, and P. M. Ajayan, "Large scale growth and characterization of atomic hexagonal boron nitride layers," Nano Lett. **10,** 3209–3215 (2010).
9. G. H. Lee, Y. J. Yu, C. Lee, C. Dean, K. L. Shepard, P. Kim, J. Hone, "Electron tunneling through atomically flat and ultrathin hexagonal boron nitride," Appl. Phys. Lett. **99,** 24311424 (2011).
10. L. Britnell, R. V. Gorbachev, R. Jalil, B. D. Belle, F. Schedin, M. I. Katsnelson, L. Eaves, S. V. Morozov, A. S. Mayorov, N. M. R. Peres, A. H. Castro Neto, J. Leist, A. K. Geim, L. A. Ponomarenko, and K. S. Novoselov, "Electron tunneling through ultrathin boron nitride crystalline barriers," Nano Lett. **12,** 1707–1710 (2012).
11. E. D. Palik, *Handbook of Optical Constants of Solids* (Academic, New York, 1985).

#259224 Received 9 Feb 2016; revised 3 Apr 2016; accepted 5 Apr 2016; published 8 Apr 2016

12. T. Holmgaard and S. I. Bozhevolnyi, "Theoretical analysis of dielectric-loaded surface plasmon-polariton waveguides," Phys. Rev. B **75,** 245405 (2007).
13. T. Holmgaard, Z. Chen, S. I. Bozhevolnyi, L. Markey, A. Dereux, A. V. Krasavin, and A. V. Zayats, "Wavelength selection by dielectric-loaded plasmonic components," Appl. Phys. Lett. **94,** 051111 (2009).
14. Z. Chen, T. Holmgaard, S. I. Bozhevolnyi, A. V. Krasavin, A. V. Zayats, L. Markey, and A. Dereux, "Wavelength-selective directional coupling with dielectric-loaded plasmonic waveguides," Opt. Lett. **34,** 310–312 (2009).
15. A. Kumar, J. Gosciniak, V. S. Volkov, S. Papaioannou, D. Kalavrouziotis, K. Vyrsokinos, J.-C. Weeber, K. Hassan, L. Markey, A. Dereux, T. Tekin, M. Waldow, D. Apostolopoulos, H. Avramopoulos, N. Pleros, and S. I. Bozhevolnyi, "Dielectric-loaded plasmonic waveguide components: Going practical," Laser Photonics Rev. **7,** 938–951 (2013).
16. J. Gosciniak, S. I. Bozhevolnyi, T. B. Andersen, V. S. Volkov, J. Kjelstrup-Hansen, L. Markey, and A. Dereux, "Thermo-optic control of dielectric-loaded plasmonic waveguide components," Opt. Express **18,** 1207–1216 (2010).
17. J. Grandidier, G. C. des Francs, S. Massenot, A. Bouhelier, L. Markey, J.-C. Weeber, C. Finot, and A. Dereux, "Gain-assisted propagation in a plasmonic waveguide at telecom wavelength," Nano Lett. **9,** 2935–2939 (2009).
18. C. Garcia, V. Coello, Z. Han, I. P. Radko, and S. I. Bozhevolnyi, "Partial loss compensation in dielectric-loaded plasmonic waveguides at near infra-red wavelengths," Opt. Express **20,** 7771–7776 (2012).
19. P. B. Johnson and R. W. Christy, "Optical constants of the noble metals," Phys. Rev. B **6,** 4370–4379 (1972).
20. S. Babar and J. H. Weaver, "Optical constants of Cu, Ag, and Au revisited," Appl. Opt. **54,** 477–481 (2015).
21. K. M. McPeak, S. V. Jayanti, S. J. P. Kress, S. Meyer, S. Iotti, A. Rossinelli, and D. J. Norris, "Plasmonic films can easily be better: rules and recipes," ACS Photonics **2,** 326–333 (2015).
22. D. F. P. Pile, T. Ogawa, D. K. Gramotnev, T. Okamoto, M. Haraguchi, M. Fukui, and S. Matsuo, "Theoretical and experimental investigation of strongly localized plasmons on triangular metal wedges for subwavelength waveguiding," Appl. Phys. Lett. **87,** 061106 (2005).
23. E. Moreno, S. G. Rodrigo, S. I. Bozhevolnyi, L. Martín-Moreno, and F. J. García-Vidal, "Guiding and focusing of electromagnetic fields with wedge plasmon polaritons," Phys. Rev. Lett. **100,** 023901 (2008).
24. A. Boltasseva, V. S. Volkov, R. B. Nielsen, E. Moreno, S. G. Rodrigo, S. I. Bozhevolnyi, "Triangular metal wedges for subwavelength plasmon-polariton guiding at telecom wavelengths," Opt. Express **16,** 5252–5260 (2008).
25. J. Takahara, S. Yamagishi, H. Taki, A. Morimoto, and T. Kobayashi, "Guiding of a one-dimensional optical beam with nanometer diameter," Opt. Lett. **7,** 475–477 (1997).

1. Introduction

Graphene is a material possessing numerous unique properties, of which unexpectedly high opacity combined with its tuneabilty by gating promises interesting applications in graphene-based optical modulators. Conventional simple transverse modulator configurations (where radiation is incident on and transmitted through a graphene layer) cannot fully utilize graphene's potential because of a very small interaction volume, i.e. the volume of the propagating radiation affected by graphene. A most straightforward way to increase interaction volume is to guide radiation to be modulated *along* graphene layer [1, 2]. This approach can be advantageously utilized in plasmonics dealing with electromagnetic modes which naturally propagate along and are greatly enhanced at the boundaries between metal and dielectric, where it is convenient to place a graphene layer. We have recently made several hybrid graphene-plasmonic modulators working at telecom wavelengths with some promise for applications [3, 4].

The purpose of this paper is to consider various plasmonic waveguide configurations and analyze their potential for graphene-based modulators. We evaluate numerically the maximum modulation depths one can achieve with the use of a single graphene layer as an absorbing material. For simplicity, in calculations we assume full graphene gating, i.e., full switch from non-absorbing to maximum absorbing state with the use of the optical Pauli blocking effect [5, 6], providing hereby the maximum value of modulation one can expect in the selected configuration.

To begin with, we consider simplified analytical estimations of the modulation depth for several basic configurations that can be considered as elementary building blocks of any plasmonic waveguide. Such analysis should reveal the main physics involved and hint on the most promising plasmonic mode for the realization of graphene-based modulators. We then

#259224 Received 9 Feb 2016; revised 3 Apr 2016; accepted 5 Apr 2016; published 8 Apr 2016

continue with accurate finite-element modelling of more complicated geometrical structures and suggest several candidates for the practical realization of modulators, which are analyzed in detail.

2. Analytic consideration

In the following, we assume that a plasmonic mode propagates in the z direction of the coordinate system. A single layer of pristine graphene covers completely the metal surface, thereby introducing additional absorption ΔW of energy of the propagating plasmonic mode. The absorption in graphene can be switched off using optical Pauli blocking [5], i.e., by graphene gating. Thus, the modulation of plasmonic mode is achieved by switching absorption in graphene on and off.

For simplicity of analytical derivations, we do not assume in our estimations any isolating layer between graphene and the metal constituting the plasmonic waveguide, even though one would need to introduce such a layer in experiments to realize graphene gating. This simplifying assumption modifies slightly the modulation value, but does not change the general description of the system and facilitates understanding of the requirements posed on the most efficient configuration.

As we explained above, we further assume that gating changes the state of graphene from maximum absorbing to completely non-absorbing, i.e. the modulation is maximum that can be achieved for the chosen configuration. In this case, the additional absorption of energy along the propagation direction Δz per time Δt induced by a graphene layer can be evaluated as [7]

$$\Delta W = \mathrm{Re}(\sigma)\Delta z\Delta t \int E_{\parallel}^2 dl, \tag{1}$$

where $\mathrm{Re}(\sigma)$ is the real part of graphene electrical conductivity, which for visible and near-infrared optical excitations approximately equals to $\mathrm{Re}(\sigma) = \frac{e^2}{4\hbar} = \frac{c\alpha}{4}$ with α being the fine-structure constant (and for far-infrared frequencies is affected by intraband contribution), and $E_{\parallel}$ is the tangential electric field on the metal surface (field in the plane of a graphene layer). The integration is done along graphene layer in the direction perpendicular to the mode propagation. For most of the considered below configurations, $E_{\parallel}$ is constant along integration direction, and Eq. (1) reduces to a simple product $\Delta W \approx \mathrm{Re}(\sigma)E_{\parallel}^2\Delta l\Delta z\Delta t$. Here Δl is either the plasmonic mode width or the length of graphene layer in the direction perpendicular to the mode propagation—depending on what is narrower. In other words, Δl is the overlap length between the graphene layer and the mode field in transversal direction. Comparing the additional absorption of energy ΔW with the energy flow W through a cross-sectional area perpendicular to the mode propagation direction, we obtain the relative mode absorption as $\Delta W/W$, and the modulation per unit length of propagation (in logarithmic dB units):

$$M = \frac{-10\log_{10}(1-\Delta W/W)}{\Delta z} \sim \frac{10}{\ln(10)}\frac{\Delta W}{W\Delta z}. \tag{2}$$

In the following subsections, we will use Eqs. (1) and (2) in order to evaluate the maximum achievable modulation for three basic geometrical configurations of graphene-based plasmonic modulators—namely, for surface plasmon polariton (SPP) mode [Fig. 1(a)] and for a mode of a metal nanowire with a graphene sheet either wrapping the waveguide [Fig. 1(b)] or touching it [Fig. 1(c)].

2.1. Surface plasmon polariton (SPP)

Surface plasmon polariton is a poorly confined plasmonic mode with most of the energy concentrated in dielectric. Moreover, the longitudinal electric-field component in dielectric

#259224 Received 9 Feb 2016; revised 3 Apr 2016; accepted 5 Apr 2016; published 8 Apr 2016

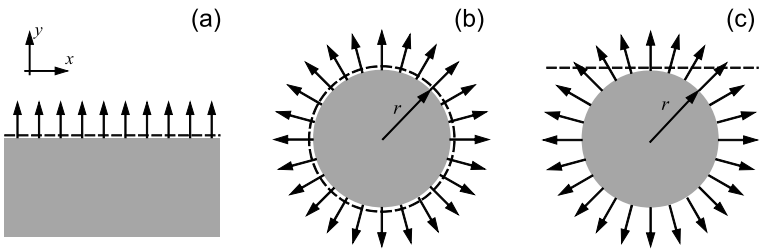

Fig. 1. Simplified geometry of three basic graphene-based plasmonic modulators: a) graphene sheet on top of a planar metal surface supporting surface plasmon polaritons; b) graphene sheet wrapping a metal nanowire; c) metal nanowire touching planar graphene sheet. Graphene is denoted by a dashed line. Assuming that plasmonic mode propagates in z direction, the arrows show transverse electric field of the waveguided mode.

is negligible (especially at telecom wavelengths) compared to transversal one [Fig. 1(a)]. Therefore, we can write the average amount of energy flow W per time Δt as follows:

$$W \approx \frac{\varepsilon_d}{8\pi} v_g \Delta t \Delta l \int_0^\infty E_\perp^2(y)dy \approx \frac{nc\Delta t \Delta l \eta}{16\pi} E_{\perp,0}^2, \tag{3}$$

where ε_d and n are material constants of dielectric, v_g is the mode group velocity, c is the speed of light, $E_{\perp,0}$ is the transversal electric field in dielectric at the surface of metal, and η is the field penetration depth in dielectric. Using Eqs. (1) and (3), we find the relative mode absorption per unit length:

$$\frac{\Delta W}{W\Delta z} = \frac{4\pi\alpha}{n\eta}\left(\frac{E_\parallel}{E_{\perp,0}}\right)^2. \tag{4}$$

Using SPP properties, we note that $\eta^{-1} = k_y = \sqrt{k_{spp}^2 - \varepsilon_d k_0^2}$ and $E_{\perp,0} = \frac{ik_{spp}}{\sqrt{k_{spp}^2 - \varepsilon_d k_0^2}} E_\parallel$, where $k_{spp} = k_0\sqrt{\varepsilon_d\varepsilon_m/(\varepsilon_d+\varepsilon_m)}$, ε_m is the real part of metal permittivity, and k_0 is the free-space k-vector. Since for visible and near-infrared wavelengths $|\varepsilon_m| \gg \varepsilon_d$, we can further simplify Eq. (4) and write the modulation M using Eq. (2) as follows:

$$M = \frac{10}{\ln(10)}\frac{8\pi^2\alpha}{\lambda}\left(\frac{\varepsilon_d}{|\varepsilon_m|}\right)^{3/2}. \tag{5}$$

For telecom wavelength $\lambda = 1.5$ μm, $\varepsilon_d \simeq 1$, and $|\varepsilon_m| \simeq 100$, we obtain $M \simeq 1.7 \times 10^{-3}$ dB/μm. This suggests that at telecom wavelength, one can realistically achieve modulation by optical Pauli blocking in graphene at the level of 0.002 dB/μm. However, the perspectives of practical applications are rather bleak, because this value is an order of magnitude lower than the intrinsic SPP attenuation due to Ohmic loss.

2.2. Cylindrical surface plasmon polariton (CySPP), full graphene wrapping

For the configuration with graphene layer wrapping a metal-nanowire waveguide [Fig. 1(b)], we can significantly simplify our derivations by considering such mode as a planar SPP mode wrapped around the nanowire. This allows us to use Eq. (4), where we again assume $E_{\perp,0} = ik_{spp}\eta E_\parallel = ik_0 N\eta E_\parallel$ with N being the mode effective index, and field penetration depth in dielectric is proportional to wavelength, $\eta = \zeta\lambda$. The dimensionless coefficient ζ depends mostly on the radius of nanowire and to lower extent on the wavelength, and varies from ~ 0.15

#259224 Received 9 Feb 2016; revised 3 Apr 2016; accepted 5 Apr 2016; published 8 Apr 2016

for a 20-nm radius to ~ 0.55 for a radius of 150 nm. Substituting the above relations into Eqs. (2) and (4), we obtain:

$$M = \frac{10}{\ln(10)} \frac{\alpha}{\pi n \lambda N^2 \zeta^3}. \tag{6}$$

For telecom wavelength range ($\lambda \simeq 1.5$ μm, $n \simeq N \simeq 1$), Eq. (6) reduces to $M \approx 6.7 \times 10^{-3} \zeta^{-3}$ dB/μm. For reasonably thick nanowires of radius 150 nm, the maximum achievable modulation is about $M \approx 0.04$ dB/μm. For much thinner nanowires of radius 20 nm, the modulation depth could reach 2 dB/μm, which is commensurable with the CySPP absorption by metal. Note that compared to the modulator based on SPP, the enhanced value of modulation M in this case is due to tighter mode confinement. This leads to enhancement of the longitudinal component of electric field, which is aligned along the graphene layer and contributes to absorption.

2.3. Cylindrical surface plasmon polariton (CySPP), flat continuous graphene sheet

In the case of a metal nanowire touching a flat graphene layer [Fig. 1(c)], the absorption of energy in graphene is given by Eq. (1), where electric field $E_{\|}$ is no longer a constant and has to be carefully integrated along the graphene layer. Contrary to the configurations considered above, the in-plane electric-field component $E_{\|}$ is the strong *transverse* CySPP field component projected on the graphene plane. For this reason, we neglect the contribution from the relatively weak longitudinal component. Assuming that $2r \leq \eta$, where r is the nanowire radius (which holds true even for μm-thick nanowires), the absorption integral in Eq. (1) evaluates to $\Delta W = \mathrm{Re}(\sigma) 2r \Delta z \Delta t E_{\perp,0}^2 K_1(\frac{2r}{\eta}) \approx \mathrm{Re}(\sigma) \eta \Delta z \Delta t E_{\perp,0}^2$, where K_1 is the modified Bessel function of the second kind. Taking this expression of absorption and the energy flow from Eq. (3) with $\Delta l = 2\pi r$ (assuming that SPP is "wrapped" around the nanowire), we obtain the maximum modulation per unit length from Eq. (2):

$$M = \frac{10}{\ln(10)} \frac{2\alpha}{nr}. \tag{7}$$

Again, calculating this value for reasonably thick nanowires of radius 150 nm in air ($n = 1$), we get an order-of-magnitude increase of modulation compared to the previous configuration: $M \approx 0.4$ dB/μm. For much thinner nanowires of radius 20 nm, the modulation depth is only slightly larger than in the wrapped CySPP configuration, $M \approx 3.2$ dB/μm, which might be because we neglected the longitudinal electric-field component, being noticeably stronger for tightly confined modes.

We note that in this last configuration, the physical contact between the graphene layer and the waveguide is substantially narrower. Nevertheless, the modulation is comparable to or sometimes substantially larger than that in the previous configurations. The latter emphasizes the importance of aligning the graphene layer along the strongest electric-field components of the mode (or at least having large projections of those), sacrificing in some cases a good wrapping of the waveguide with graphene. This somewhat counter-intuitive result might help us finding optimum configurations for a graphene-based plasmonic modulator.

3. Numeric modelling of basic structures

After establishing the main features of three basic plasmonic modulators, we are going to take a closer and more precise look at them as well as at one additional structure, which is difficult to study analytically—dielectric-loaded surface plasmon polariton waveguide (DLSPPW). It is necessary to note that we simplified the geometry of structures in the previous section, and assumed that graphene layer touches the metal surface of the waveguide, whereas graphene

#259224 Received 9 Feb 2016; revised 3 Apr 2016; accepted 5 Apr 2016; published 8 Apr 2016

gating requires a dielectric spacer between them. The presence of such spacer moves graphene away from the enhanced electric fields of a plasmonic waveguide and can strongly reduce the achievable modulation depth. Therefore, in this section we consider precise finite-element method (FEM) modelling of the same structures where we introduced an isolating layer of hexagonal boron nitride (hBN). The choice of this material is governed by its large resistivity, good elastic properties, high breakdown field strength, and a feasibility to fabricate atomically-flat layers [8–10]—properties that make hBN a good candidate as a dielectric in capacitors, and hence for graphene gating.

As a first configuration, we consider SPP propagating along a gold–air interface. A single atomic layer of graphene spans the gold surface through a layer of hBN, whose thickness is a variable parameter in simulations. Overall, the considered configuration is a four-layer structure: gold–hBN–graphene–air without gaps between layers. In simulations (accomplished using COMSOL Multiphysics), we do not create a medium corresponding to graphene, because introducing material (macroscopic) parameters for a single atomic layer cannot be fully justified. Instead, to accurately take absorption in graphene into account, we calculate the mode-field distribution, and, similar to Eq. (1), integrate the value $\mathrm{Re}(\sigma)E_{\parallel}^2$ over hBN–air interface (cf. supplementary information in [7]). For evaluation of energy flow W, we also use the calculated mode-field distribution and group velocity in the form $v_g = c/(N - \lambda \frac{\partial N}{\partial \lambda})$, where N is the effective mode index and λ is the free-space wavelength. We accomplish all the following simulations and evaluation of achievable modulation depth using the same procedure. For the refractive index of hBN, we take the value of 1.8, whereas the gold permittivity value is taken from Palik [11]. All numerical simulations are done for a fixed telecom wavelength of 1500 nm.

The results of simulations for SPP mode show a presence of modulation maximum for a particular hBN thickness [Fig. 2(a,b)]. For the selected wavelength of 1500 nm, it lies at around 180 nm. One can understand the existence of the maximum from the following reasoning. For a very large thickness of hBN layer, the considered mode resembles a mode of SPP at an interface of two semi-infinite gold and hBN media, whose field decays exponentially away from the interface. Therefore, the field at hBN–air interface (where the graphene layer is applied) is low, and so is the modulation. With a decrease of hBN thickness, the mode undergoes compression and is partially pushed inside the metal, which results in increased loss. At the same time, the modulation grows as well, because progressively more energy is stored inside hBN layer, and the field at hBN–air interface and inside graphene increases. At a certain thickness of hBN, the energy of the mode can no longer be stored inside it, and with the further decrease of hBN thickness, the field is pushed out into air. This leads to a decrease of the field in graphene and therefore to a decreased modulation depth. The loss decreases as well, because part of the mode energy redistributes from metal into air. This primitive description explains also the proximity of modulation and mode loss maxima: They have the same physical origin.

From the graph on Fig. 2(b), one can also see that the mode loss is quantitatively larger than modulation depth at the most of hBN thicknesses. There, however, exists an interval of thicknesses ($\sim$ 100–200 nm), at which modulation is larger than loss, and the dominance of modulation is maximum at the middle of the interval (at $\sim$ 150 nm of hBN thickness), where it exceeds loss by slightly more than 10%. This configuration due to its simplicity might be interesting for practical applications.

Another configuration worth being considered is DLSPPW mode, because it provides a much more practical laterally confined mode with good propagation length [12]. Moreover, a large set of passive and a few active plasmonic components have been developed for this geometry [13–18]. Similar to the previous structure, we introduce a layer of hBN of variable thickness on top of the gold surface, beneath the dielectric waveguide made of acrylic glass (PMMA), whose

#259224 Received 9 Feb 2016; revised 3 Apr 2016; accepted 5 Apr 2016; published 8 Apr 2016

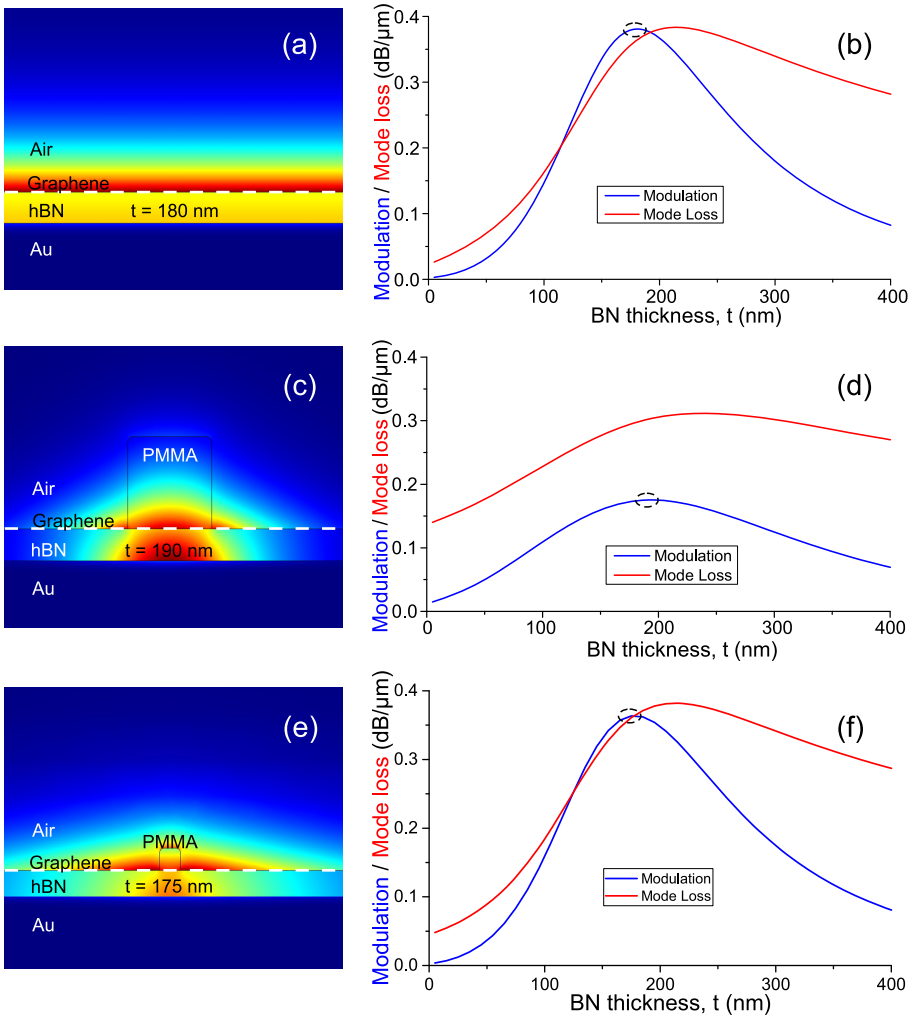

Fig. 2. Modelling of modulation depth and mode loss for graphene-based devices exploiting (a),(b) surface plasmon polariton (SPP) and (c),(d),(e),(f) dielectric-loaded SPP waveguide (DLSPPW) modes. In finite-element method (FEM) calculations, the thickness *t* of the isolating layer — hexagonal boron nitride (hBN) — was the varying parameter. Electric-field plots (a),(c), and (e) show field amplitude distribution for the case of hBN thickness that gives maximum modulation depth in the corresponding configuration [denoted by dashed circles on panels (b) and (d)]. White dashed lines on field plots denote the location of graphene layer. Dimensions of the DLSPPW are as follows: (c) width – 500 nm, height – 550 nm, (e) width – 140 nm, height – 150 nm.

#259224
Received 9 Feb 2016; revised 3 Apr 2016; accepted 5 Apr 2016; published 8 Apr 2016

geometry is optimized for mode confinement at telecom wavelength [12]: 500 nm in width and 550 nm in height [Fig. 2(c)]. Again, we simulate the graphene layer on top of hBN medium below the PMMA waveguide.

As in the case of the regular SPP mode, the dependencies of the DLSPPW mode loss and modulation depth on the hBN thickness show a maximum at around 200 nm (235 nm for loss and 195 nm for modulation), which is of the same physical origin [Fig. 2(d)]. However, several features are substantially different from those observed for the SPP mode. One can see that for very small (or absent, as the limiting case) thicknesses of hBN, the modulation is noticeably higher exceeding that of the SPP mode by a factor of 5. This is indeed expected, as DLSPPW mode is well confined, and hence have larger longitudinal component of electric field, which contributes to absorption in graphene. This advantage is quickly lost though with an increase of hBN thickness, because the mode loses its confinement, and the modulation at its maximum has considerably lower value. Contrary to the SPP mode, modulation depth of the DLSPPW mode never exceeds absorption. This last result is disappointing, as well as somewhat unexpected, but can be attributed to the deterioration of the mode profile through the introduction of a planar layer of isolating medium, i.e., the whole idea of introducing a layer of hBN spoils the DLSPPW mode structure.

We would also like to briefly consider how geometrical parameters of the DLSPPW affect the modulation depth with respect to intrinsic mode loss. One can immediately notice that decreasing the waveguide width and/or height gradually converts DLSPPW mode into planar SPP by decreasing the mode lateral confinement. In this respect, there is no optimum width of the waveguide that maximizes the modulation: The modulation gradually increases with decreasing the DLSPPW width to zero. In practice, however, the width of the waveguide is roughly limited by its height, as it is hard to fabricate tall narrow polymer ridges with aspect ratio below one. Thus, for any given DLSPPW height, it is most reasonable to use a waveguide with aspect ratio close to unity, and one is faced with the usual for plasmonics trade-off between mode confinement and any other useful property (modulation in our case). As an example, we provide the results of numerical modelling of a scaled-down DLSPPW of 140 nm in width and 150 nm in height [Fig. 2(e,f)]. Comparing with the previous DLSPPW, one can see that the mode became substantially broader, and the dependences of modulation depth and mode loss on hBN thickness resemble those of the SPP mode.

Let us now consider a mode of metal nanowire with two possible wrappings by a graphene layer: (*i*) fully wrapped configuration and (*ii*) a nanowire on a planar surface. In both configurations, a layer of hBN (either wrapped or planar) of variable thickness isolates graphene sheet from the metal structure. Another variable parameter in the modelling is the radius of the nanowire. A fully wrapped configuration is hardly feasible in experimental implementation and is only interesting from theoretical point of view as an elementary building block for more complicated geometries. For this reason and for the sake of easier comparison with other configurations, we will use material parameters of gold for the metal structure, even though for a practical realization of plasmonic metal-nanowire waveguide, silver would be a better choice. Precise FEM modelling of the structure with the smallest reasonable radius of the nanowire (20 nm) and thickness of hBN layer varying from 5 to 100 nm gives a tightly confined mode [Fig. 3(b)] and dependencies of modulation depth and mode loss versus hBN thickness [Fig. 3(a)] very similar to those obtained for regular SPP mode [Fig. 2(b)]. With a sweep of the hBN thickness, both quantities feature a maximum, which are reached at close thicknesses of the isolating layer (55 and 85 nm, respectively). One can notice though that the values of modulation and absorption are an order of magnitude larger than those for the SPP mode, and that the modulation depth never exceeds loss. With an increase of the nanowire radius, this quasi-resonant dependence gets wider, whereas the absolute values of modulation

#259224 Received 9 Feb 2016; revised 3 Apr 2016; accepted 5 Apr 2016; published 8 Apr 2016

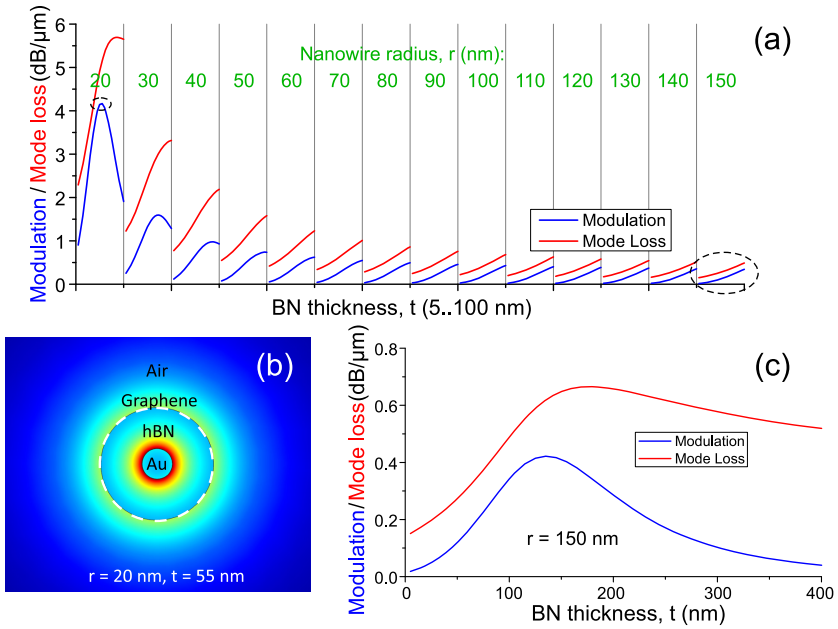

Fig. 3. (a) Modelling of modulation depth and mode loss for graphene-based device exploiting a mode of gold nanowire with graphene layer fully wrapping the waveguide. The variable parameters in the FEM calculations are nanowire radius r changing from 20 to 150 nm with a step of 10 nm and hBN thickness t, varying from 5 to 100 nm for each radius. (b) Electric-field plot for the geometry, giving the maximum modulation: $r = 20$ nm, $t = 55$ nm [denoted by a dashed circle in panel (a)]. White dashed line denotes the location of graphene layer. (c) Calculated mode loss and modulation depth for $r = 150$ nm and an extended range of hBN thicknesses [denoted by a dashed circle in panel (a)].

and loss decrease and should finally converge to the case of the flat SPP mode. Simulation for a wider range of hBN thicknesses for the largest nanowire radius (150 nm) shows that the modulation and loss curves never cross each other [Fig. 3(c)] in the whole range of the considered nanowire radii. This is a result of unfortunate trade-off between the extent of plasmonic mode confinement and the degree of overlap between the graphene layer and the electric field. Indeed, better mode confinement produces stronger longitudinal electric field, which is favorable for modulation. On the other hand, tighter confinement leaves less possibility for graphene to probe the electric field due to the isolation layer.

Even though the tightly confined mode of a metal nanowire provides an enhanced longitudinal (axial) electric-field component, the transversal (radial) component of electric field is substantially stronger in the dielectric part of the waveguide. In the fully wrapped metal-nanowire configuration, the graphene layer is always exactly perpendicular to the strongest electric field component and cannot fully exploit the potential of this mode. This disadvantage is alleviated to some extent in the case of the nanowire on top of a planar surface [Fig. 4(b,c)], where most of the transverse electric-field lines have a projection on the graphene plane, though the geometrical overlap is substantially smaller. We have already pointed this out in the first section during approximate analytical consideration of the structure. In more precise numerical FEM modelling, we take into account the hBN planar isolating layer. Moreover, to make the structure more realistic, we assume that the whole geometry resides on a glass substrate. Our simulations reveal some interesting details of this configuration [Fig. 4(a)].

#259224 Received 9 Feb 2016; revised 3 Apr 2016; accepted 5 Apr 2016; published 8 Apr 2016

Contrary to the previous geometries, there is no optimum thickness of the isolating layer: The dependencies of modulation depth and mode loss on hBN thickness are monotonous curves without extrema, with the minimum (ideally, zero) thickness giving the best conditions, i.e., maximum modulation at the minimum mode loss. Interestingly, for the smallest and several largest considered radii of the nanowire ($r = 20$ nm and $r \geq 100$ nm), modulation exceeds loss for isolating layer thicknesses below $\sim$ 10–15 nm, which are feasible in experiment. It is important to note that depending on the fabrication conditions, the same structure with gold substituted by silver can provide considerably lower absorption in metal and moderately lower confinement [19–21], which will result in both lower mode loss and higher modulation depth, making hereby this geometry more attractive.

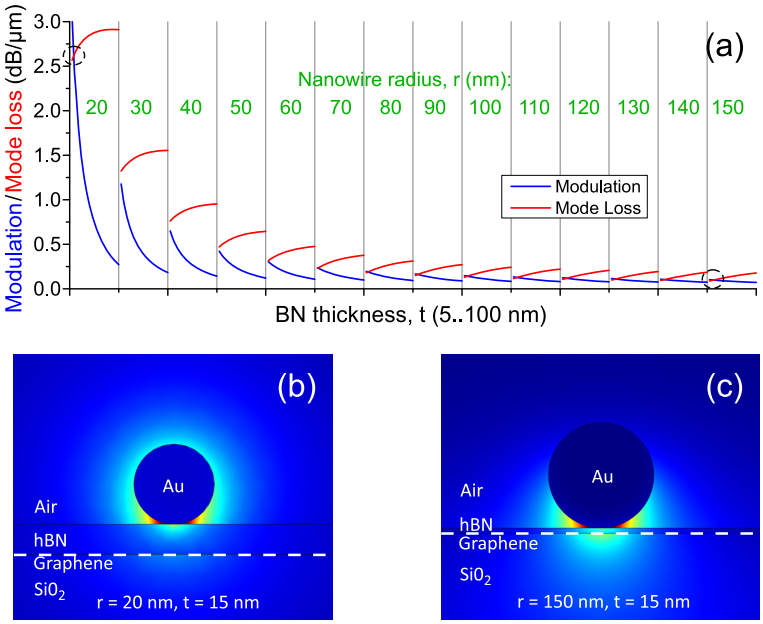

Fig. 4. (a) Modelling of modulation depth and mode loss for graphene-based device exploiting a mode of gold nanowire with a planar graphene sheet below the isolating layer of hBN. The variable parameters in the FEM calculations are nanowire radius r changing from 20 to 150 nm with a step of 10 nm and hBN thickness t, varying from 5 to 100 nm for each radius. (b),(c) Electric-field plots for two geometries [denoted by dashed circles in panel (a)] yielding the modulation depth, which is comparable to intrinsic mode loss: (b) $r = 20$ nm, $t = 15$ nm and (c) $r = 150$ nm, $t = 15$ nm. White dashed lines on field plots denote the location of graphene layer.

4. Modelling edge-based waveguides

We have established in the previous section that among various basic plasmonic waveguiding modes, the mode of a metal nanowire under certain conditions is the most promising for modulation by absorption in graphene. The main condition to be fulfilled is that the electric field that drives electrons in graphene and hence being absorbed must be primarily the mode's transversal component, rather than its generally week longitudinal one. This can be guaranteed by finding a proper geometry of the waveguide and/or the way graphene is introduced into the system. The latter can be especially challenging if one aims at an experimentally feasible configuration, not imposing very hard limits on the fabrication procedure. In this section, we

#259224 Received 9 Feb 2016; revised 3 Apr 2016; accepted 5 Apr 2016; published 8 Apr 2016

will investigate three waveguides that bear similarity with the above-mentioned mode of the nanowire, but provide more flexibility in fabrication and allow easier integration with other nano-optic components, such as in- and out-couplers, passive waveguiding components, other waveguiding structures, etc.

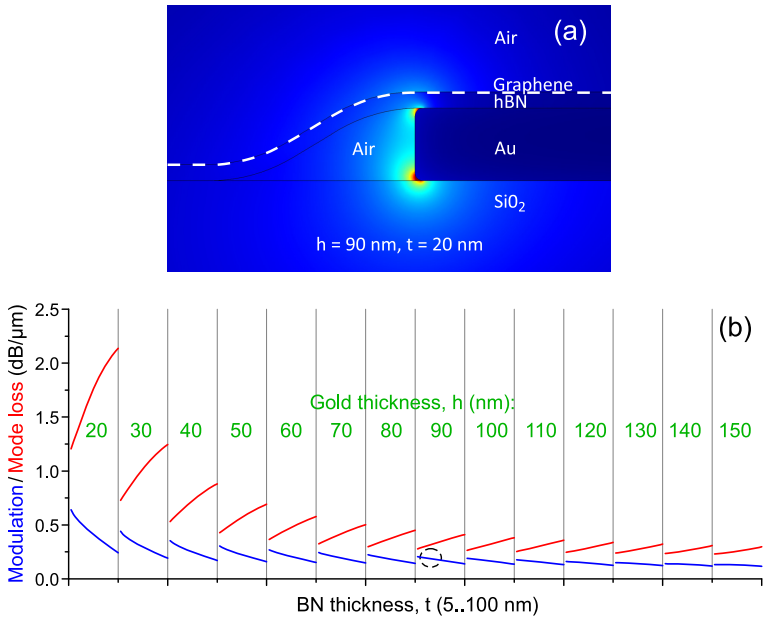

Fig. 5. Graphene-based modulator based on edge plasmon mode: Spatially limited planar gold film deposited on a dielectric substrate supports a plasmonic mode bound to its edge, whereas graphene flake covers the edge through an isolation layer of hBN. The variable parameters in the FEM calculations are gold-film thickness *h* changing from 20 to 150 nm with a step of 10 nm and hBN thickness *t*, varying from 5 to 100 nm for each value of *h*. Smooth wrapping of the edge with a hBN layer is approximated by an s-curve with two bends of radius 200 nm. The gold-edge corners are rounded by a curvature of 10-nm radius. a) Modeled electric-field distribution of plasmonic edge mode supported by a gold film of thickness 90 nm covered with a 20-nm-thick layer of hBN. White dashed line denotes the location of graphene layer. b) Calculated mode modulation (blue curves) and loss (red curves) for a set of geometrical parameters: Gold thickness varies from 20 to 150 nm with a step of 10 nm, and for each gold-film thickness, the thickness of hBN varies from 5 to 100 nm.

Metallic edges, both planar and in the form of a wedge, are known to support a confined propagating surface plasmon mode, which is very similar to the mode of a nanowire in that its field has axial symmetry [22–24] along the curved part of the edge. Thus, a gold stripe with smooth edges or just an edge of a large planar structure (e.g., a film) can guide a spatially confined plasmonic mode. Fabrication of such a waveguide and subsequent covering with layers of hBN and graphene should be relatively easy, and provide a good approximation to the configuration described in the previous section. Indeed, in the assumption that a graphene sheet on top of an hBN layer covers a gold-film edge fabricated on a glass substrate, the FEM modelling results [Fig. 5] resemble those of a metal nanowire waveguide [Fig. 4]. The absolute values of the mode loss decreased approximately by half [Fig. 5(b)] due to lower confinement of the mode, since it partially spans the flat parts of the metal surface. However, the decrease of the modulation depth is more pronounced, so that the modulation is lower than the mode

#259224 Received 9 Feb 2016; revised 3 Apr 2016; accepted 5 Apr 2016; published 8 Apr 2016

loss for any combination of gold and hBN thicknesses. One can easily understand this drop of efficiency by noticing that the modulator utilizes only half of the space [the left half on Fig. 5(a)] of the geometry, whereas the right part of metallic structure is a planar film without curvature and hence does not participate in modulation.

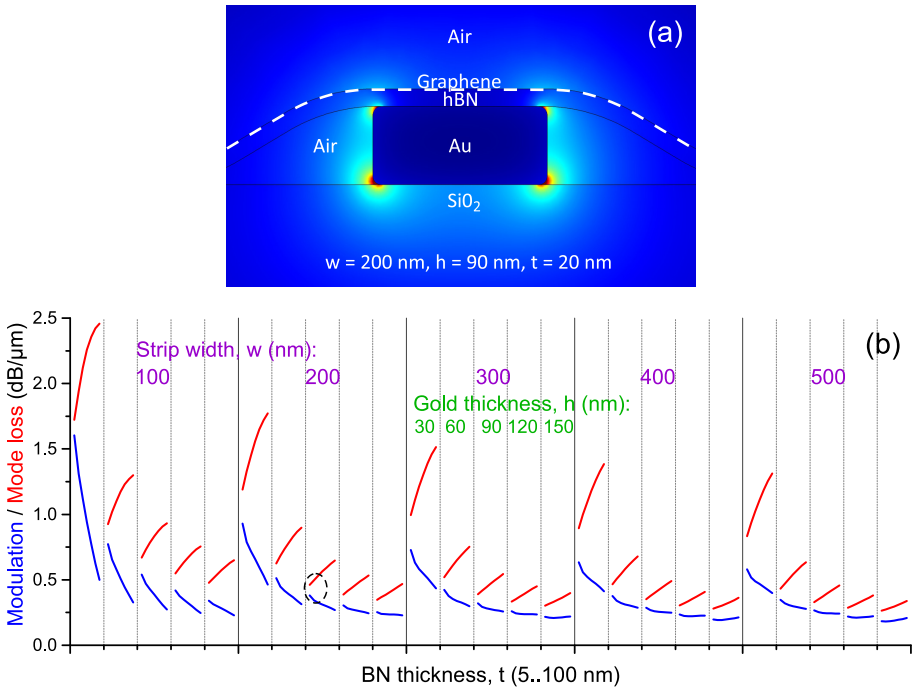

Fig. 6. Graphene-based modulator based on strip plasmon mode: a gold strip supported by a dielectric substrate and covered by a graphene flake through an isolation layer of BN. The parameters of hBN bending and rounded corners of the gold are the same as in Fig. 5. a) Modeled electric-field distribution of plasmonic strip mode supported by a gold waveguide of thickness 90 nm and width 200 nm covered with a 20-nm-thick layer of hBN. White dashed line denotes the location of graphene layer. b) Calculated mode modulation depth (blue curves) and intrinsic loss (red curves) for a set of geometrical parameters: gold thickness varies from 30 to 150 nm with a step of 30 nm, and for each gold-film thickness, the thickness of hBN varies from 5 to 100 nm. Each set of gold and hBN thicknesses is considered for the strip width changing from 100 to 500 nm with a step of 100 nm.

The latter disadvantage can be eliminated by supplementing the left edge with a completely symmetric right one, making hereby a stripe waveguide with a graphene surface absorbing the mode's energy doubled [Fig. 6(a)]. As expected in this case, the gap between modulation and loss curves decreases, bringing those values close to each other. Varying the stripe width and metal-film thickness, one can tune parameters of the mode, such as propagation length, confinement (and hence bend loss), and efficiency of modulation [Fig. 6(b)]. As in previous cases, however, the decisive parameter in determining the modulation depth relative to the mode loss is the thickness of the isolating hBN layer. It should be as thin as possible to decrease the intrinsic mode absorption in metal and to bring its absorption in graphene to maximum.

In order to fully explore the potential of edge-based plasmonic waveguides, we have to consider geometry complementary to a stripe, i.e. a slot waveguide [Fig. 7(a)]. This structure has similar to a stripe waveguide physical contact with graphene, because there are also two

#259224 Received 9 Feb 2016; revised 3 Apr 2016; accepted 5 Apr 2016; published 8 Apr 2016

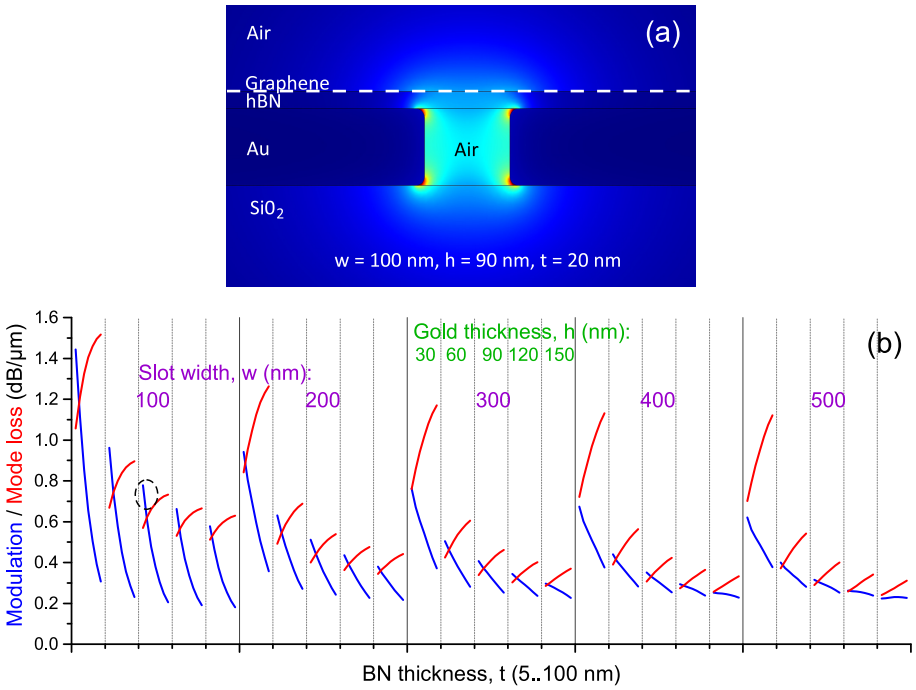

Fig. 7. Graphene-based modulator based on slot plasmon mode: a slot cut through a gold film supported by a dielectric substrate and covered by a graphene flake through an isolating layer of hBN. Corners of the gold edge are rounded by a curve of 10-nm radius. a) Modelled electric-field distribution of plasmonic slot mode supported by a slot width 100 nm cut in gold film of thickness 90 nm covered with a 20-nm-thick layer of hBN. White dashed line denotes the location of graphene layer. b) Calculated mode modulation depth (blue curves) and intrinsic loss (red curves) for a set of geometrical parameters: gold thickness varies from 30 to 150 nm with a step of 30 nm, and for each gold-film thickness, the thickness of hBN varies from 5 to 100 nm. Each set of gold and hBN thicknesses is considered for the slot width changing from 100 to 500 nm with a step of 100 nm.

edges contributing with transversal electric-field components into interaction. However, if the slot between the two edges is narrow enough, the electric-field lines are more homogeneous and aligned horizontally across the gap, parallel to the plane of graphene. This should result in an increase of the modulation depth relative to mode absorption. Our FEM simulations of the slot waveguide with the slot width, gold-film and hBN thicknesses being the variable parameters, confirm these conclusions [Fig. 7(b)]. For the hBN thickness below 15–20 nm, most of the combinations of the slot width and gold thickness yield a modulation depth, which is higher than the intrinsic mode loss. One can also notice from the graphs for 200- and 300-nm-wide slots that the gold film should not be too thin, neither too thick, i.e., there is an interval of optimum thickness. One can understand this again by considering the field in the gap between edges. When the gold layer is too thin, the field in the gap is very inhomogeneous and therefore its alignment with graphene plane is poor. Contrary, when the gold-film thickness is too large, the gap resembles an efficient capacitor with most of the field concentrated inside the gap, so that at the plane of graphene, which is above and outside the gap, the field has mostly proper orientation, but is very weak.

We would like to point out that we used 10-nm rounding for metal edges in the described

#259224
Received 9 Feb 2016; revised 3 Apr 2016; accepted 5 Apr 2016; published 8 Apr 2016

waveguides. While this number is commonly used in modelling of plasmonic structures, the edge sharpness can hardly be controlled during fabrication. Fortunately, losses of edge-based modes (which are similar to the mode of metal nanowire) grow faster than modulation depth does with the decrease of radius of edge curvature. The latter can be understood by extremely fast (super-exponential) and infinite grows of mode absorption in metal nanowire with its vanishing radius [25]. This means that waveguides with larger radii of edge rounding should show modulation properties superior to those presented in this section.

5. Conclusions

In summary, we have considered analytically several very basic surface plasmon waveguiding configurations and investigated their potential for the realization of graphene-based plasmonic modulators, which exploit absorption in graphene, tunable through the optical Pauli blocking effect. While it is in general very difficult to obtain modulation depth values larger than intrinsic mode loss, we showed that for the efficient modulation, electric currents in graphene have to be driven primarily by the transversal electric-field component of the modulated plasmonic mode, and therefore it is crucial to guarantee its large projection onto the graphene plane. Contrary, the longitudinal electric-field component is too weak to induce appreciable mode absorption in graphene, even when being perfectly aligned with its plane. The latter applies to both poorly and very tightly confined plasmonic modes, i.e., universally applicable to all plasmonic configurations.

Having established this, we performed accurate FEM modelling of seven plasmonic configurations operating at telecom wavelengths, for which we carefully took into account the details of geometry, such as the necessary presence of an isolating layer between metal and graphene, rounded corners of metallic structures, and realistic (i.e., feasible in experiment) wrapping of structures with graphene layer. Among all considered configurations, we found a particularly promising one, with which it is possible to achieve modulation depth that exceeds the intrinsic mode loss. Even though the available set of surface-plasmon waveguides is very rich and not limited by the considered structures, one can analyze or approximate those not discussed in this work by one of our basic configurations. They represent the building blocks reflecting the main features of other waveguides in terms of mode confinement, mode-field symmetry, geometrical shape, used materials, etc. We therefore believe that our results can help in consideration and designing of novel active-plasmonic modulators that exploit graphene as a medium with controllably variable absorption.

Acknowledgments

The authors acknowledge the financial support from the Danish Council for Independent Research (the FTP project ANAP, Contract No. 09-072949), from the European Research Council, Grant No. 341054 (PLAQNAP), and from SAIT GRO Program, EPSRC grant EP/K011022/1, Bluestone Global Inc. Grant, E.C. Graphene Flagship grant (contract no. CNECT-ICT-604391).

#259224 Received 9 Feb 2016; revised 3 Apr 2016; accepted 5 Apr 2016; published 8 Apr 2016